

March 8, 2022



# Osoyoos Lake, Washington

## Topobathymetric Lidar Technical Data Report

*Prepared For:*



**International Joint Commission**  
Washington Office  
1717 H Street NW, Suite 835  
Washington, DC 20006  
PH: 202-736-9000

*Prepared By:*



**NV5 Geospatial Corvallis**  
1100 NE Circle Blvd, Ste. 126  
Corvallis, OR 97330  
PH: 541-752-1204



# TABLE OF CONTENTS

INTRODUCTION .....	1
Deliverable Products .....	2
ACQUISITION .....	4
Planning.....	4
Turbidity Measurements and Secchi Depth Readings .....	4
Airborne Survey .....	7
Lidar.....	7
Digital Imagery .....	10
Ground Survey .....	11
Base Stations .....	11
Ground Survey Points (GSPs) .....	11
Aerial Targets .....	12
Land Cover Class.....	12
PROCESSING .....	15
Topobathymetric Lidar Data .....	15
Bathymetric Refraction .....	18
Lidar Derived Products.....	18
Topobathymetric DEMs .....	18
Digital Imagery .....	19
RESULTS & DISCUSSION .....	20
Bathymetric Lidar.....	20
Mapped Bathymetry and Depth Penetration .....	20
Lidar Point Density .....	22
First Return Point Density .....	22
Bathymetric and Ground Classified Point Densities.....	22
Lidar Accuracy Assessments.....	24
Lidar Non-Vegetated Vertical Accuracy .....	24
Lidar Bathymetric Vertical Accuracies.....	27
Lidar Vegetated Vertical Accuracies.....	29
Lidar Relative Vertical Accuracy .....	31
Lidar Horizontal Accuracy.....	32
Photo Analytical Aerial Triangulation Report.....	33
Overview .....	33
Control Points.....	33
Check Points.....	34
Anomalies and Misfits .....	34
CERTIFICATIONS.....	35
SELECTED IMAGES.....	36
GLOSSARY .....	37
APPENDIX A - ACCURACY CONTROLS.....	38

**Cover Photo:** A photo taken by NV5 staff shows a scenic view looking over the Osoyoos Lake project area.

# INTRODUCTION

This photo taken by NV5 acquisition staff shows a view of the Enloe Dam Powerhouse on the Similkameen River in the Osoyoos Lake site in Washington.



In September 2021, NV5 Geospatial (NV5) was contracted by the International Joint Commission, U.S. Section (IJC) to collect topobathymetric Light Detection and Ranging (lidar) data and digital imagery in the late summer and early fall of 2021 for the Osoyoos Lake site in Washington. The Osoyoos Lake area of interest covers the southern US portion of Osoyoos Lake, and adjacent portion of the Okanagan and Similkameen Rivers. Traditional near-infrared (NIR) lidar was fully integrated with green wavelength return data (bathymetric) lidar in order to provide a seamless topobathymetric lidar dataset. Topobathymetric lidar data were collected to aid IJC in assessing infrastructure planning, risk mitigation, and help improve flood mapping, and hydrodynamic modelling.

This report accompanies the delivered topobathymetric lidar data and imagery, and documents contract specifications, data acquisition procedures, processing methods, and analysis of the final dataset including lidar accuracy, depth penetration, and density. Acquisition dates and acreage are shown in Table 1, a complete list of contracted deliverables provided to IJC is shown in Table 2, and the project extent is shown in Figure 1.

**Table 1: Acquisition dates, acreage, and data types collected on the Osoyoos Lake site**

Project Site	Project Area Square Kilometers	Acquisition Dates	Data Type
Osoyoos Lake, Washington	23.30	09/14/2021	Topobathymetric Lidar
		09/16/2021	4 band (RGB-NIR) Digital Imagery

# Deliverable Products

**Table 2: Products delivered to IJC for the Osoyoos Lake site**

<b>Osoyoos Lake Lidar Products</b> <b>Projection: UTM Zone 11 North</b> <b>Horizontal Datum: NAD83 (2011)</b> <b>Vertical Datum: NAVD88 (GEOID18)</b> <b>Units: Meters</b>	
<b>Topobathymetric Lidar</b>	
<b>Points</b>	LAZ v 1.4 PF6 <ul style="list-style-type: none"> <li>• Raw Swaths</li> <li>• All Classified Returns</li> <li>• Ground and Bathymetric Bottom Classified Returns</li> </ul>
<b>Rasters</b>	1.0 Meter Cloud Optimized GeoTiffs <ul style="list-style-type: none"> <li>• Void Clipped Topobathymetric Bare Earth Digital Elevation Model (DEM)</li> </ul>
<b>Vectors</b>	Shapefiles (*.shp) <ul style="list-style-type: none"> <li>• Area of Interest</li> <li>• Lidar Tile Index</li> <li>• DEM Tile Index</li> <li>• Bathymetric Coverage Shape**</li> <li>• Water’s Edge Breaklines</li> <li>• Ground Survey Points</li> </ul>
<b>4 Band (RGBI) Digital Imagery</b>	
<b>Rasters</b>	10 cm GeoTiffs <ul style="list-style-type: none"> <li>• Tiled Imagery Mosaics</li> </ul> 10 cm MrSID Compression <ul style="list-style-type: none"> <li>• AOI Imagery Mosaic</li> </ul>
<b>Vectors</b>	Shapefiles <ul style="list-style-type: none"> <li>• Tile Index</li> <li>• Area of Interest</li> <li>• Air Target Points</li> </ul>

*\*\*NV5 delivered these Lidar-derived products in addition to contracted deliverables in order to provide a more complete and versatile dataset to IJC.*

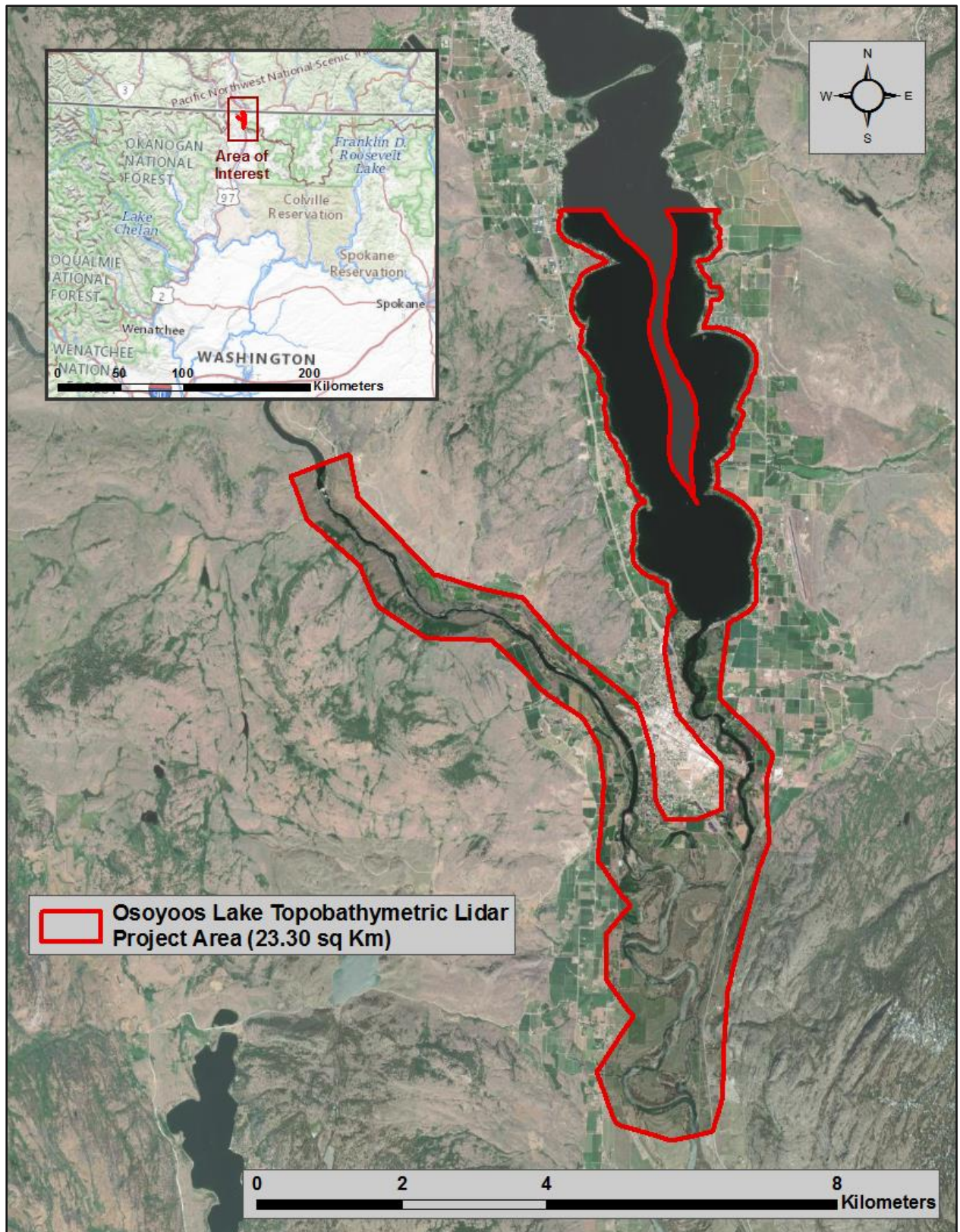


Figure 1: Location map of the Osoyoos Lake site in Washington

## ACQUISITION

NV5's ground acquisition equipment set up over monument 79C438 in the Osoyoos Lake Lidar study area.



### Planning

In preparation for data collection, NV5 reviewed the project area and developed a specialized flight plan to ensure complete coverage of the Osoyoos Lake Lidar study area at the target combined point density of  $\geq 4$  points/m<sup>2</sup>. Acquisition parameters including orientation relative to terrain, flight altitude, pulse rate, scan angle, and ground speed were adapted to optimize flight paths and flight times while meeting all contract specifications.

Factors such as satellite constellation availability and weather windows must be considered during the planning stage. Any weather hazards or conditions affecting the flight were continuously monitored due to their potential impact on the daily success of airborne and ground operations. In addition, logistical considerations including private property access, potential air space restrictions, and water clarity were reviewed.

### Turbidity Measurements and Secchi Depth Readings

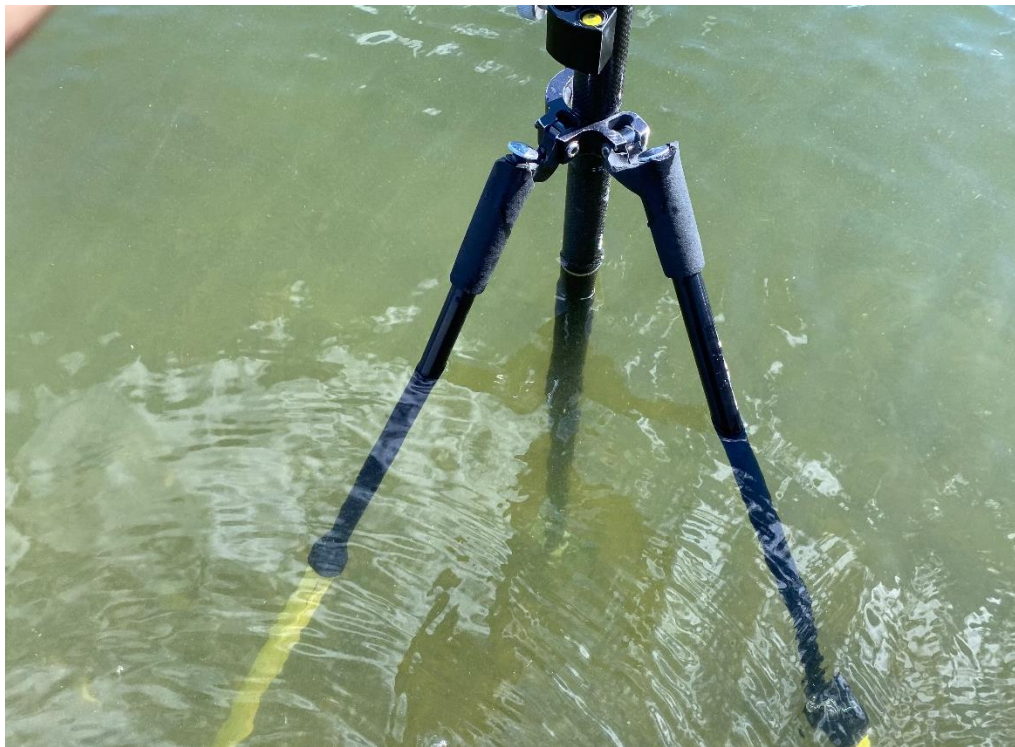
In order to assess water clarity conditions prior to and during lidar and digital imagery collection, NV5 collected turbidity measurements, secchi depth readings, and weather observations. Readings were collected at three throughout the project site on September 14, 2021. Turbidity measurements were recorded three times at each location to confirm measurements. The table below provides turbidity and secchi depth results per site on the day of data collection.

**Table 3: Water Clarity Observations for Lidar flights**

Turbidity, Secchi Depth, and Wind Speed Observations						
Date	Time	Location	Turbidity Read 1 (NTUs)	Turbidity Read 2 (NTUs)	Turbidity Read 3 (NTUs)	*Secchi Depth (m)
9/14/21	9:25	TURB_19	8.15	7.94	7.73	0.80 m
9/14/21	16:00	TURB_20	0.31	0.28	0.35	3.75 m
9/14/21	17:05	TURB_21	0.37	0.48	0.45	1.10 m

**Table 4: Secchi Depth and Turbidity Locations. Coordinates are in the NAD83 (2011) datum, UTM Zone 11N**

Secchi Depth and Turbidity Locations				
Location	X	Y	Z	Reading Type
TURB_19	327848.710	5541182.070	426.104	Secchi Depth and Turbidity
TURB_20	321281.814	5434689.361	279.343	Secchi Depth and Turbidity
TURB_21	321785.014	5431718.657	279.424	Secchi Depth and Turbidity



*NV5 field survey photos showing water clarity conditions and ground survey equipment set up over submerged shallow water targets at two location within the Okanagan Lakes Area of Interest.*

# Airborne Survey

## Lidar

The lidar survey was accomplished using a Leica Chiroptera/Hawkeye 4X shallow green, deep green, and NIR laser system mounted in a Cessna Caravan. The green wavelength ( $\lambda=532$  nm) laser is capable of collecting high resolution topography data, as well as penetrating the water surface with minimal spectral absorption by water. The NIR wavelength laser ( $\lambda=1064$  nm) that adds additional topography data and aids in water surface modeling. The recorded waveform enables range measurements for all discernible targets for a given pulse. The typical number of returns digitized from a single pulse range from 1 to 7 for the Osoyoos Lake project area. It is not uncommon for some types of surfaces (e.g., dense vegetation or water) to return fewer pulses to the lidar sensor than the laser originally emitted. The discrepancy between first return and overall delivered density will vary depending on terrain, land cover, and the prevalence of water bodies. All discernible laser returns were processed for the output dataset. Table 5 summarizes the settings used to yield an average pulse density of  $\geq 4$  pulses/m<sup>2</sup> over the Osoyoos Lake project area.

All areas were surveyed with an opposing flight line side-lap of  $\geq 20\%$  ( $\geq 40\%$  overlap) in order to reduce laser shadowing and increase surface laser painting. To accurately solve for laser point position (geographic coordinates x, y and z), the positional coordinates of the airborne sensor and the attitude of the aircraft were recorded continuously throughout the lidar data collection mission. Position of the aircraft was measured twice per second (2 Hz) by an onboard differential GPS unit, and aircraft attitude was measured 200 times per second (200 Hz) as pitch, roll and yaw (heading) from an onboard inertial measurement unit (IMU). To allow for post-processing correction and calibration, aircraft and sensor position and attitude data are indexed by GPS time.



*Leica Chiroptera CH4X and HawkEye  
HE4X Lidar Sensor System*

**Table 5: Lidar specifications and survey settings**

Lidar Survey Settings & Specifications			
Acquisition Dates	09/14/2021		
Aircraft Used	Cessna Caravan		
Sensor	Leica		
Laser	Chiroptera 4X NIR	Chiroptera 4X Green	Hawkeye 4X Green
Maximum Returns	15	15	15
Resolution/Density	Average 4 pulses/m <sup>2</sup>	Average 4 pulses/m <sup>2</sup>	Average 4 pulses/m <sup>2</sup>
Nominal Pulse Spacing	0.50 m	0.50 m	0.50 m
Survey Altitude (AGL)	500 m	500 m	500 m
Survey speed	145 knots	145 knots	145 knots
Field of View	40°	40°	40°
Scan Frequency	37 Rotations Per Second	37 Rotations Per Second	37 Rotations Per Second
Target Pulse Rate	250 kHz	35 kHz	10 kHz
Pulse Length	2.5 ns	2.5 ns	2.0 ns
Laser Pulse Footprint Diameter	0.1 m	1.6 m	2.88 m
Central Wavelength	1,064 nm	515 nm	515 nm
Pulse Mode	Multiple Pulses in Air	Multiple Pulses in Air	Multiple Pulses in Air
Beam Divergence	0.25 mrad	4 mrad	7.2 mrad
Swath Width	364 m	364m	364m
Swath Overlap	25%	25%	25%
Intensity	16-bit	16-bit	16-bit
Accuracy	RMSE <sub>z</sub> (Non-Vegetated) ≤ 20 cm		
	NVA (95% Confidence Level) ≤ 39.2 cm		
	VVA (95 <sup>th</sup> Percentile) ≤ 60 cm		

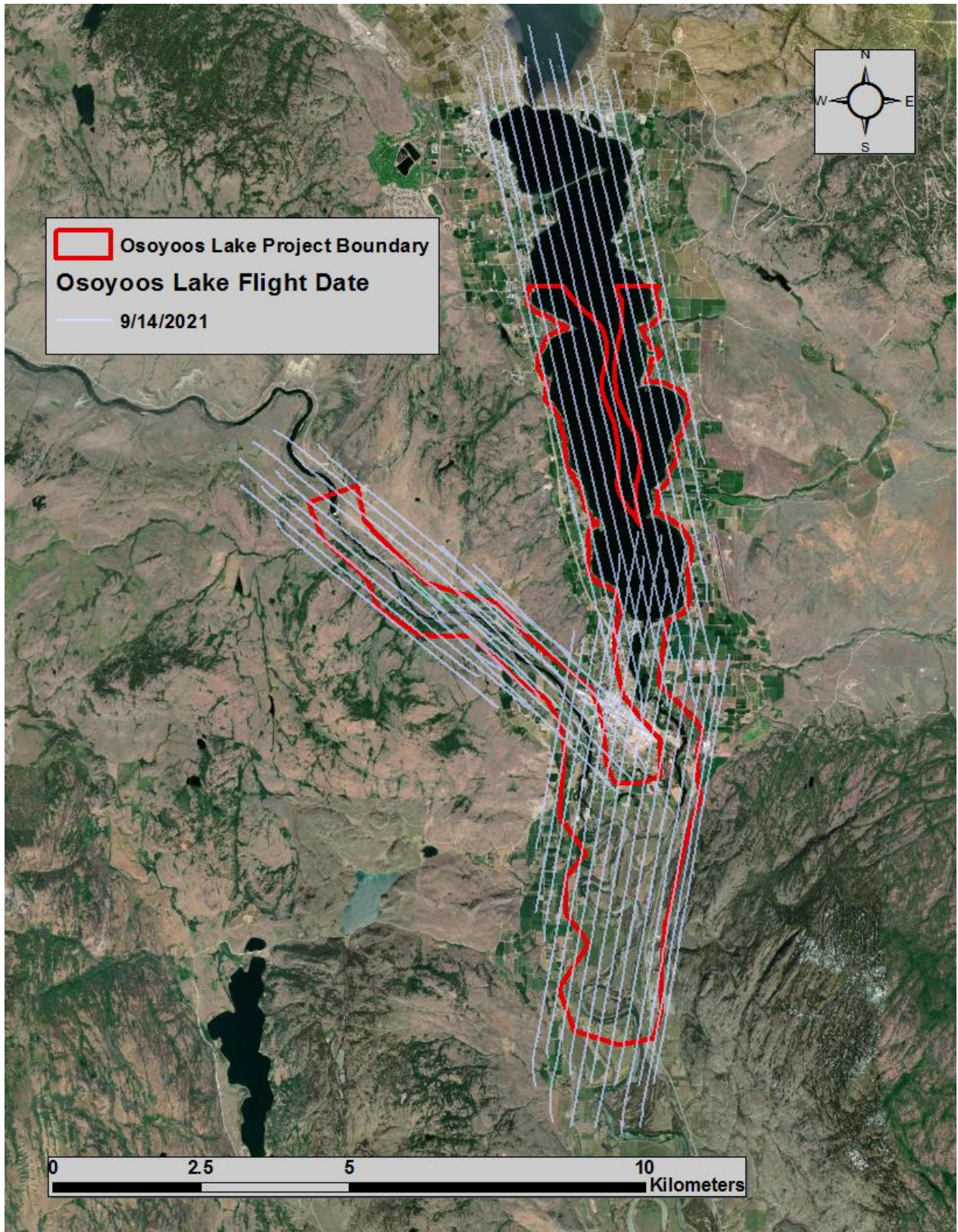


Figure 2: Flightline Index Map

## Digital Imagery

Aerial imagery was collected by Peregrine Aerial Surveys using a DMC III digital mapping camera (Table 5). The DMC III is a large format, aerial camera manufactured by Leica. The system is gyro-stabilized and simultaneously collects panchromatic and multispectral (RGB, NIR) imagery.

**Table 5: Camera manufacturer’s specifications**

DMC III	
Focal Length	92 mm
Spectral Bands	RGB NIR
Pixel Size	3.9 $\mu$ m
Image Size	25,728 x 14,592 pixels
Frame Rate	1.8 seconds
FOV	57° x 34°
Date Format	8bit TIFF

For the Osoyoos Lake site, 87 images were collected with 60% along track overlap and 30% sidelap between frames. The acquisition flight parameters were designed to yield a native pixel resolution of  $\leq$  10 cm. Orthophoto specifications particular to the Osoyoos Lake project are in Table 6.

**Table 6: Project-specific orthophoto specifications**

Digital Orthophotography Specifications	
Ground Sampling Distance (GSD)	$\leq$ 10 cm pixel size
Along Track Overlap	$\geq$ 60%
Cross Track Overlap	$\geq$ 30%
Height Above Ground Level (AGL)	2,200 m
GPS PDOP	$\leq$ 3.0
GPS Satellite Constellation	$\geq$ 6

## Ground Survey

Ground control surveys, including monumentation, aerial targets and ground survey points (GSPs), were conducted by NV5 ground survey staff to support the airborne acquisition. Ground control data were used to geospatially correct the aircraft positional coordinate data and to perform quality assurance checks on final lidar data and orthoimagery products.

### Base Stations

Monuments were used for collection of ground survey points using real time kinematic (RTK), fast static (FS), and total station (TS) survey techniques.

Base station locations were selected with consideration for satellite visibility, field crew safety, and optimal location for GSP coverage. NV5 utilized one existing NR Canada benchmark and established one new monument for the Osoyoos Lake Lidar project (Table 6, Figure 3). New monumentation was set using 5/8" x 30" rebar topped with stamped 2 1/2" aluminum caps. NV5's professional land surveyor, Evon Silvia oversaw the ground survey work for the project.

**Table 6: Monument positions for the Osoyoos Lake acquisition. Coordinates are on the NAD83 (2011) datum, epoch 2010.00**

Monument ID	Location	Type	Latitude	Longitude	Ellipsoid (meters)
79C438	British Columbia	NRCAN BM	49° 00' 33.32652"	-119° 24' 40.07234"	553.934
OBWB_06	Washington	NV5	49 00' 33.32755"	-119 24' 47.92311"	272.862

NV5 utilized static Global Navigation Satellite System (GNSS) data collected at 1 Hz recording frequency for each base station. Multiple independent sessions over the same monument were processed to confirm antenna height measurements and to refine position accuracy.

### Ground Survey Points (GSPs)

Ground survey points were collected using real time kinematic (RTK) and fast-static (FS) survey techniques. For RTK surveys, a roving receiver receives corrections from a nearby base station or Real-Time Network (RTN) via radio or cellular network, enabling rapid collection of points with relative errors less than 1.5 cm horizontal and 2.0 cm vertical. FS surveys compute these corrections during post-processing to achieve comparable accuracy. RTK surveys record data while stationary for at least five seconds, calculating the position using at least three one-second epochs. FS surveys record observations for up to fifteen minutes on each GSP in order to support longer baselines. All GSP measurements were made during periods with a Position Dilution of Precision (PDOP) of  $\leq 3.0$  with at least six satellites in view of the stationary and roving receivers. See Table 7 for NV5 ground survey equipment information.

Forested check points are collected using total stations in order to measure positions under dense canopy. Total station backsight and setup points are established using GNSS survey techniques.

GSPs were collected in areas where good satellite visibility was achieved on paved roads and other hard surfaces such as gravel or packed dirt roads. GSP measurements were not taken on highly reflective

surfaces such as center line stripes or lane markings on roads due to the increased noise seen in the laser returns over these surfaces. GSPs were collected within as many flightlines as possible; however, the distribution of GSPs depended on ground access constraints and monument locations and may not be equitably distributed throughout the study area (Figure 3).

**Table 7: NV5 Geospatial ground survey equipment identification**

Receiver Model	Antenna	OPUS Antenna ID	Use
Trimble R7	Zephyr GNSS Geodetic Model 2 RoHS	TRM57971.00	Static
Trimble R10 Model 2	Integrated Antenna	TRMR10-2	Rover
Trimble R12	Integrated Antenna	TRMR12	Rover
Nikon NPL-322+ 5" P Total Station		n/a	VVA
Trimble M3 Total Station		n/a	VVA



## Aerial Targets

Air target points (ATP) were collected throughout the project area prior to imagery acquisition to refine the exterior orientation parameters of the camera and conduct an accuracy assessment of the final orthophoto product. ATPs are typically collected over hard surface ground features or temporary vinyl chevrons. Hard surface points consist of high contrast, road markings such as stop bars and turn arrows and cement corners. Typically each corner of the road marking is surveyed, in this way only one point was used for aerial triangulation while the remaining points are used for quality assurance purposes. Each ATP was surveyed using Fast Static (FS) or RTK techniques.

## Land Cover Class

In addition to ground survey points, land cover class check points were collected throughout the study area to evaluate vertical accuracy. Vertical accuracy statistics were calculated for all land cover types to assess confidence in the lidar derived ground models across land cover classes (Table 8, see Lidar Accuracy Assessments, page 24).

**Table 8: Land Cover Types and Descriptions**

Land Cover Type	Land Cover Code	Example	Description	Accuracy Assessment Type
Shrubbery	SH		Rangeland dominated by shrub and brush	VVA
Tall Grass	TG		Herbaceous grasslands in advanced stages of growth	VVA
Mixed Forest	FR		Forested areas dominated by mixed deciduous, and coniferous species	VVA
Bare Earth	BE		Areas of bare earth surface	NVA
Urban	UA		Areas dominated by urban development, including parks	NVA

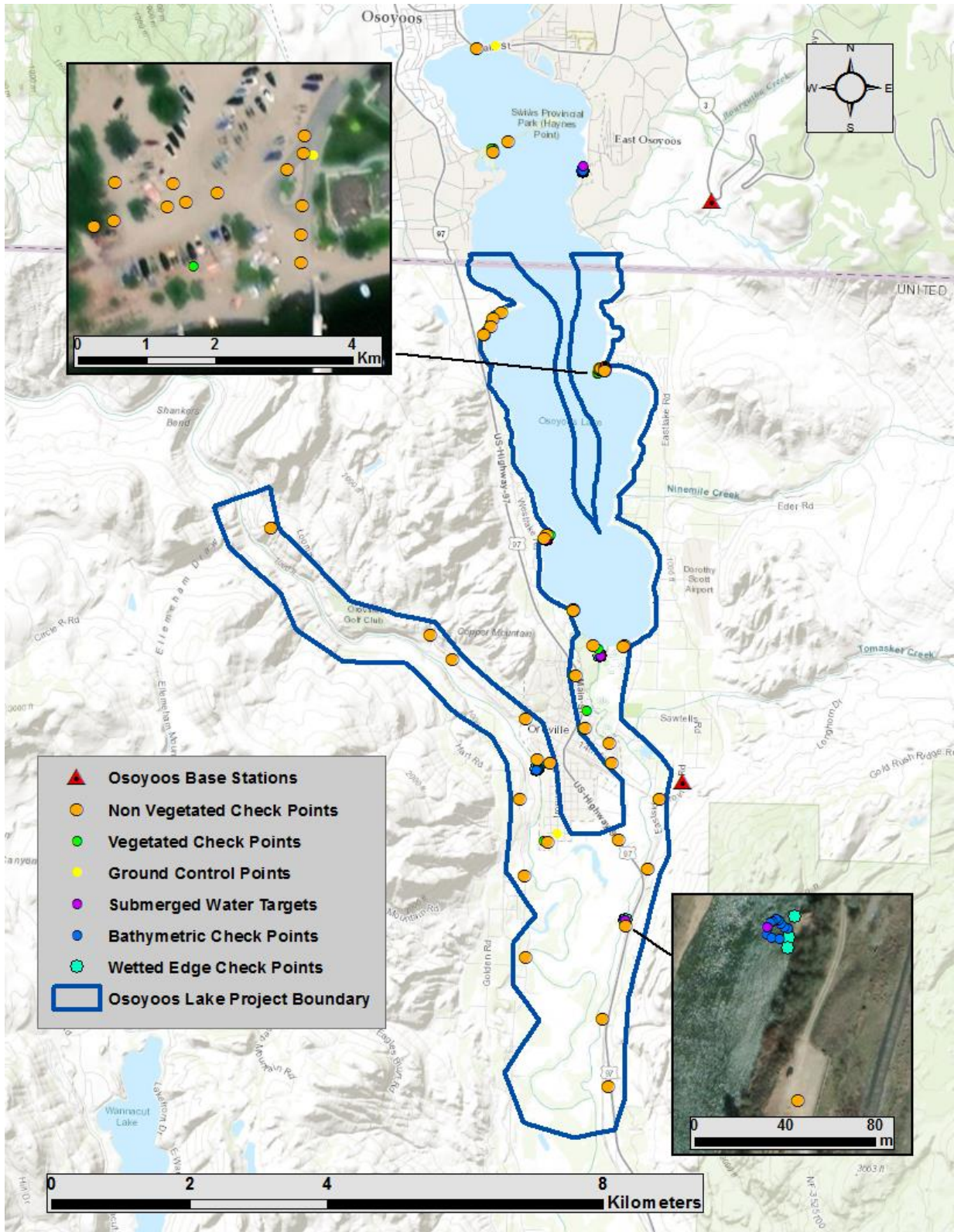
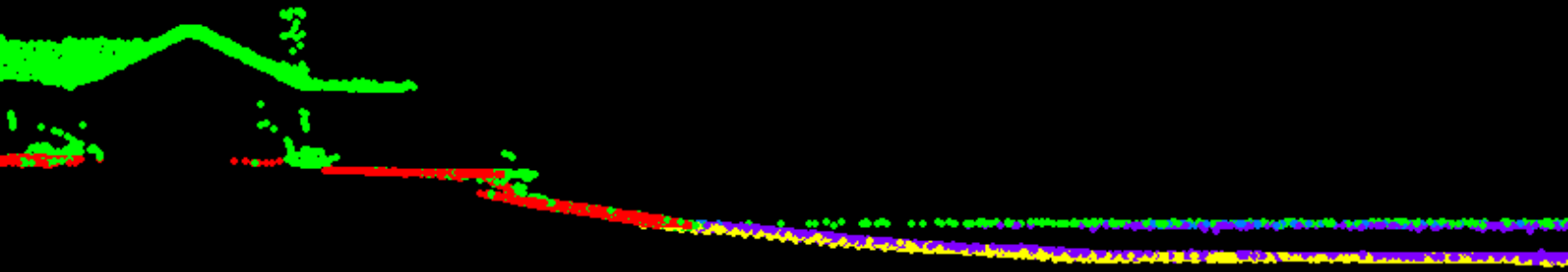
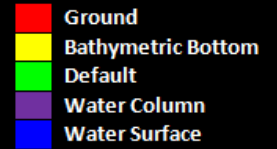


Figure 3: Ground survey location map

## PROCESSING

This 6 meter lidar cross section shows a view of the Osoyoos Lake landscape, colored by point classification



### Topobathymetric Lidar Data

Upon completion of data acquisition, NV5 processing staff initiated a suite of automated and manual techniques to process the data into the requested deliverables. Processing tasks included GPS control computations, smoothed best estimate trajectory (SBET) calculations, kinematic corrections, calculation of laser point position, sensor and data calibration for optimal relative and absolute accuracy, and lidar point classification (Table 9).

Bathymetric refraction corrections were then applied using Las Monkey (NV5 Geospatial proprietary software). The resulting point cloud data were classified using both manual and automated techniques. Processing methodologies were tailored for the landscape. Brief descriptions of these tasks are shown in Table 10.

**Table 9: ASPRS LAS classification standards applied to the Osoyoos Lake dataset**

Classification Number	Classification Name	Classification Description
1	Default/Unclassified	Laser returns that are not included in the ground class, composed of vegetation and anthropogenic features
2	Ground	Laser returns that are determined to be ground using automated and manual cleaning algorithms
7	NIR Laser Noise	NIR laser returns that are often associated with birds, scattering from reflective surfaces, or artificial points below the ground surface
9	NIR Laser Water Surface	NIR laser returns that are determined to be water using automated and manual cleaning algorithms
40	Bathymetric Bottom	Refracted green laser returns that fall within the water's edge breakline which characterize the submerged topography.
41	Green Laser Water Surface	Green laser returns that are determined to be water surface points using automated and manual cleaning algorithms.
45	Water Column	Refracted green laser returns that are determined to be water using automated and manual cleaning algorithms.
47	Green Laser Noise	Green laser returns that are often associated with birds, scattering from reflective surfaces, or artificial points below the bathymetric surface

**Table 10: Lidar processing workflow**

Lidar Processing Step	Software Used
Resolve kinematic corrections for aircraft position data using kinematic aircraft GPS, PPP and static ground GPS data. Develop a smoothed best estimate of trajectory (SBET) file that blends post-processed aircraft position with sensor head position and attitude recorded throughout the survey.	Waypoint Inertial Explorer v.8.9
Calculate laser point position by associating SBET position to each laser point return time, scan angle, intensity, etc. Create raw laser point cloud data for the entire survey in *.las (ASPRS v. 1.4) format. Convert data to orthometric elevations by applying a geoid correction.	Lidar Survey Studio v.3.0.1 LasProjector v.1.3 (NV5 Proprietary Software)
Import raw laser points into manageable blocks to perform manual relative accuracy calibration and filter erroneous points. Classify ground points for individual flight lines.	TerraScan v.19
Using ground classified points per each flight line, test the relative accuracy. Perform automated line-to-line calibrations for system attitude parameters (pitch, roll, heading), mirror flex (scale) and GPS/IMU drift. Calculate calibrations on ground classified points from paired flight lines and apply results to all points in a flight line. Use every flight line for relative accuracy calibration.	BayesMap StripAlign v.2.19 TerraMatch v.19
Apply refraction correction to all subsurface returns.	Las Monkey 2.6 (NV5 proprietary software)
Classify resulting data to ground and other client designated ASPRS classifications (Table 9). Assess statistical absolute accuracy via direct comparisons of ground classified points to ground control survey data.	TerraScan v.19 TerraModeler v.19
Generate bare earth models as triangulated surfaces. Export all surface models as Cloud Optimized GeoTiffs(.tif) format at a 1 meter pixel resolution.	TerraScan v.19 TerraModeler v.19 Las Product Creator 3.0 (NV5 proprietary software) ArcMap v. 10.3.1
Correct intensity values for depth.	Las Monkey 2.6 (NV5 proprietary software)

## Bathymetric Refraction

Green lidar pulses that enter the water column must have their position corrected for refraction of the light beam as it passes through the water and its resulting decreased speed and change in direction. Las Monkey (NV5 proprietary software) was used to perform this correction based on Snell's law, using the information on the sensor's position from the SBET and a model of the water surface. The water surface model (WSM) was developed using the point cloud from the NIR sensor and information from water's edge survey points. The Osoyoos Lake area used a fixed elevation model, while the Okanagan River and Similkameen River areas used NIR points within the breaklines defining the water's edge. Points were filtered and edited to obtain the most accurate representation of the water surface and are used to create a water surface model TIN. A TIN model is preferable to a raster based water surface model to obtain the most accurate angle of incidence during refraction.

The Las Monkey software intersects the partially submerged green pulse vectors with the WSM to determine the angle of incidence with the water surface and the submerged component of the pulse vector. This provides the information necessary to correct the position of underwater points by adjusting the submerged vector length and angle. After refraction, the points are compared against bathymetric check points to assess accuracy.

## Lidar Derived Products

Because hydrographic laser scanners penetrate the water surface to map submerged topography, this affects how the data should be processed and presented in derived products from the lidar point cloud. The following discusses certain derived products that vary from the traditional (NIR) specification and delivery format.

## Topobathymetric DEMs

Creating digital elevation models (DEMs) presents a challenge with respect to interpolation of areas with no returns. Traditional DEMs are "unclipped", meaning areas lacking ground returns are interpolated from neighboring ground returns, with the assumption that the interpolation is close to reality. In bathymetric modeling, these assumptions are prone to error because a lack of bathymetric returns can indicate a change in elevation that the laser can no longer map due to increased depths. The resulting void areas may suggest greater depths, rather than similar elevations from neighboring bathymetric bottom returns. Therefore, NV5 Geospatial created a polygon of bathymetric voids to delineate areas outside of successfully mapped bathymetry. This shapefile was used to control the extent of the delivered clipped topobathymetric model and to avoid false triangulation across areas in the water with no returns.

## Digital Imagery

As with the lidar, the collected digital photographs went through multiple processing steps to create final orthophoto products. Initially, images were corrected for geometric distortion to yield level02 image files. Next, images were color balanced and levels were adjusted to exploit the full 14bit histogram and finally output as level03 pan-sharpened 8bit TIFF images. Camera position and orientation were calculated by linking the time of image capture to the smoothed best estimate of trajectory (SBET). Within Inpho’s Match AT softcopy photogrammetric software, analytical aerial triangulation was performed using ground control, automatically generated tie points, and camera calibration information.

Adjusted images were orthorectified using the Lidar-derived ground model to remove displacement effects from topographic relief inherent in the imagery. The resulting orthos were mosaicked within Inpho’s OrthoVista blending seams and applying automated project color-balancing. The final mosaics were inspected and edited for seam cutlines across above ground features such as buildings and other man-made features. Special care was taken to eliminate glare on the water surface. The processing workflow for orthophotos is summarized in Table 11.

**Table 11: Orthophoto processing workflow**

Orthophoto Processing Step	Software Used
Resolve GPS kinematic corrections for the aircraft position data using kinematic aircraft GPS (collected at 2 Hz) and PPP data.	Waypoint Inertial Explorer v.8.9
Develop a smooth best estimate trajectory (SBET) file that blends post-processed aircraft position with attitude data. Sensor heading, position, and attitude are calculated throughout the survey.	Waypoint Inertial Explorer v.8.9
Create an exterior orientation file (EO) for each photo image with omega, phi, and kappa.	Waypoint Inertial Explorer v.8.9
Convert Level 00 raw imagery data into geometrically corrected Level 02 image files.	HxMap
Apply radiometric adjustments to Level 02 image files to create Level 03 Pan-sharpened TIFFs.	HxMap
Apply EO to photos, measure ground control points and perform aerial triangulation.	Inpho Match AT v10.0.2
Import DEM and orthorectify image frames	Inpho OrthoMaster v10.0.2
Mosaic orthorectified imagery blending automated and manually drawn seams between photos and applying global color balancing to the project.	Inpho OrthoVista/Seameditor v10.0.2

This 2 meter LiDAR cross section shows a view of vegetation and bare ground in the Osoyoos Lake AOI, colored by point laser echo.

Only Echo  
First of Many  
Intermediate  
Last of Many

### Bathymetric Lidar

An underlying principle for collecting hydrographic lidar data is to survey near-shore areas that can be difficult to collect with other methods, such as multi-beam sonar, particularly over large areas. In order to determine the capability and effectiveness of the bathymetric lidar, several parameters were considered; depth penetrations below the water surface, bathymetric return density, and spatial accuracy.

### Mapped Bathymetry and Depth Penetration

To assist in evaluating performance results of the sensor, a polygon layer was created to delineate areas where bathymetry was successfully mapped.

This shapefile was used to control the extent of the delivered clipped topo-bathymetric model and to avoid false triangulation across areas in the water with no returns. Insufficiently mapped areas were identified by triangulating bathymetric bottom points with an edge length maximum of 4.56 meters. This ensured all areas of no returns ( $> 9 \text{ m}^2$ ), were identified as data voids. Overall NV5 successfully mapped 45% of the bathymetric bottom within the project area.

**Table 12: Depth Penetration Statistics**

Absolute Vertical Accuracy		
Depth	Area M <sup>2</sup>	Percent
Shallow	1,013,620	25.1%
0.1 - 1m	452,887	11.2%
1 - 2m	995,460	24.7%
2 - 3m	623,724	15.5%
3 - 4m	342,868	8.5%
4 - 5m	302,435	7.5%
5 - 6m	255,821	6.3%
> 6m	44,669	1.1%
	4,031,484	100%

# Lidar Point Density

## First Return Point Density

The acquisition parameters were designed to acquire an average first-return density of 4 points/m<sup>2</sup>. First return density describes the density of pulses emitted from the laser that return at least one echo to the system. Multiple returns from a single pulse were not considered in first return density analysis. Some types of surfaces (e.g., breaks in terrain, water and steep slopes) may have returned fewer pulses than originally emitted by the laser.

First returns typically reflect off the highest feature on the landscape within the footprint of the pulse. In forested or urban areas the highest feature could be a tree, building or power line, while in areas of unobstructed ground, the first return will be the only echo and represents the bare earth surface.

The average first-return density of the Osoyoos Lake Lidar project was 13.95 points/m<sup>2</sup> (Table 13). The statistical distributions of all first return densities per 100 m x 100 m boundary clipped cells are portrayed in Figure 4.

## Bathymetric and Ground Classified Point Densities

The density of ground classified lidar returns and bathymetric bottom returns were also analyzed for this project. Terrain character, land cover, and ground surface reflectivity all influenced the density of ground surface returns. In vegetated areas, fewer pulses may have penetrated the canopy, resulting in lower ground density. Similarly, the density of bathymetric bottom returns was influenced by turbidity, depth, and bottom surface reflectivity. In turbid areas, fewer pulses may have penetrated the water surface, resulting in lower bathymetric density.

The ground and bathymetric bottom classified density of lidar data for the Osoyoos Lake project was 6.52 points/m<sup>2</sup>(Table 13). The statistical distributions ground classified and bathymetric bottom return densities per 100 m x 100 m boundary clipped cells are portrayed in Figure 5.

Additionally, for the Osoyoos Lake project, density values of only bathymetric bottom returns were calculated for areas containing at least one bathymetric bottom return. Areas lacking bathymetric returns (voids) were not considered in calculating an average density value. Within the successfully mapped area, a bathymetric bottom return density of 4.84 points/m<sup>2</sup> was achieved.

**Table 13: Average Lidar point densities**

Density Type	Point Density
First Returns	13.95 points/m <sup>2</sup>
Ground and Bathymetric Bottom Classified Returns	6.52 points/m <sup>2</sup>
Bathymetric Bottom Classified Returns	4.84 points/m <sup>2</sup>

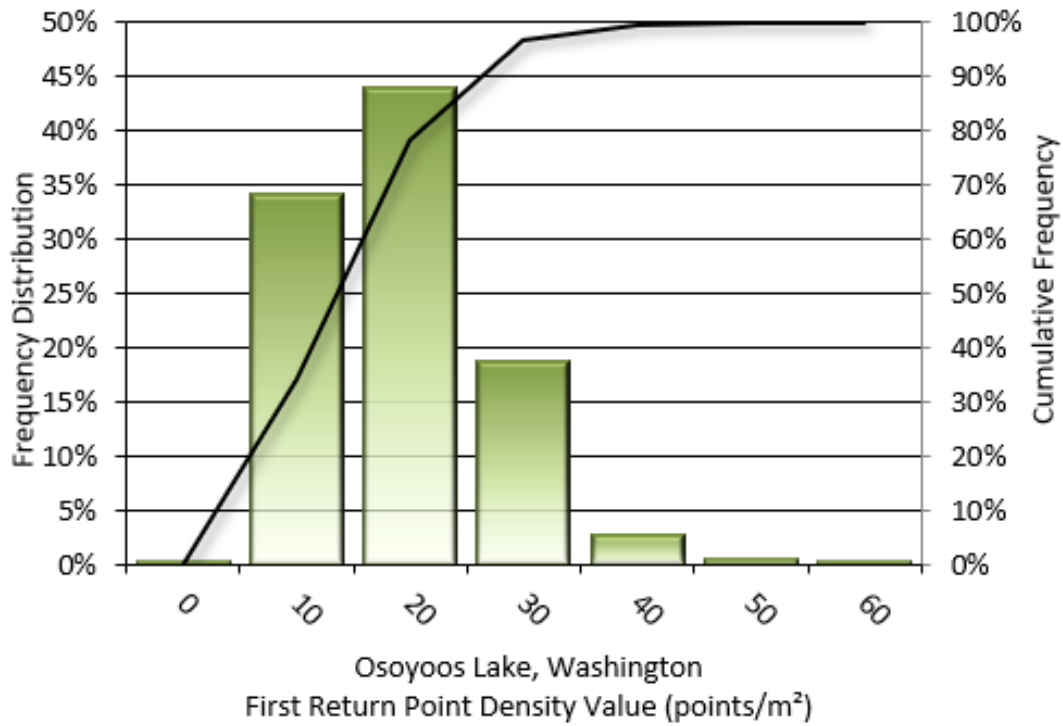


Figure 4: Frequency distribution of first return densities per 100 x 100 m cell

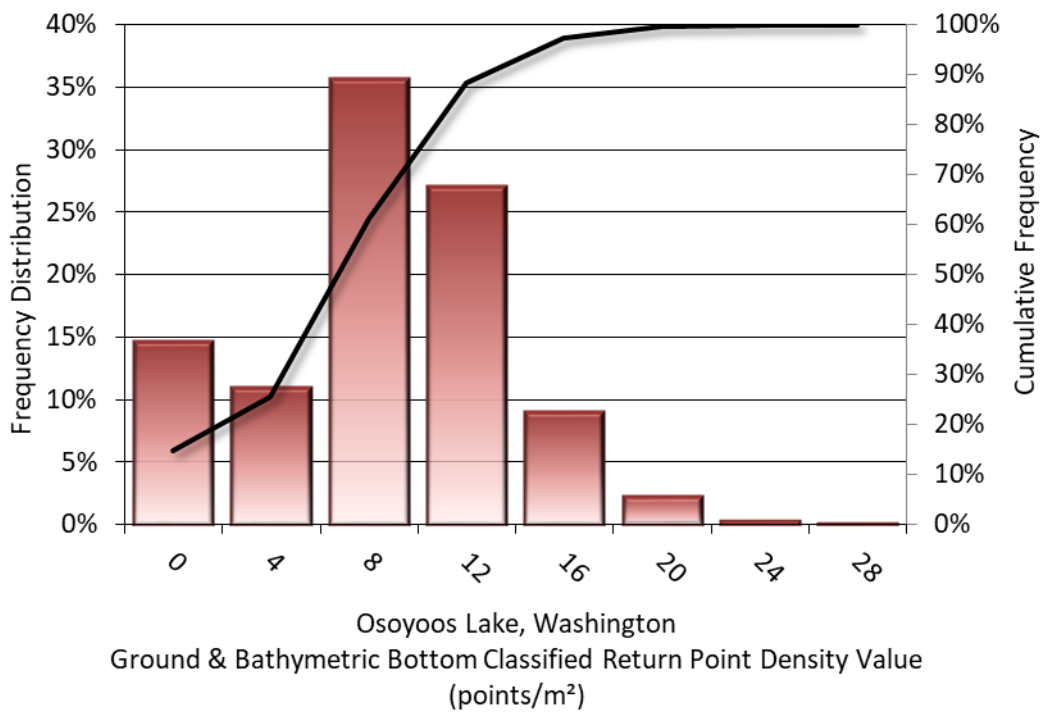


Figure 5: Frequency distribution of ground and bathymetric bottom classified return densities per 100 x 100 m cell

## Lidar Accuracy Assessments

The accuracy of the lidar data collection can be described in terms of absolute accuracy (the consistency of the data with external data sources) and relative accuracy (the consistency of the dataset with itself). See Appendix A for further information on sources of error and operational measures used to improve relative accuracy.

### Lidar Non-Vegetated Vertical Accuracy

Absolute accuracy was assessed using Non-vegetated Vertical Accuracy (NVA) reporting designed to meet guidelines presented in the FGDC National Standard for Spatial Data Accuracy<sup>1</sup>. NVA compares known ground check point data that were withheld from the calibration and post-processing of the lidar point cloud to the triangulated surface generated by the classified lidar point cloud as well as the derived gridded bare earth DEM. NVA is a measure of the accuracy of lidar point data in open areas where the lidar system has a high probability of measuring the ground surface and is evaluated at the 95% confidence interval ( $1.96 * RMSE$ ), as shown in Table 14.

The mean and standard deviation (sigma  $\sigma$ ) of divergence of the ground surface model from ground check point coordinates are also considered during accuracy assessment. These statistics assume the error for x, y and z is normally distributed, and therefore the skew and kurtosis of distributions are also considered when evaluating error statistics. For the Osoyoos Lake survey, 48 ground check points were withheld from the calibration and post-processing of the lidar point cloud, with resulting non-vegetated vertical accuracy of 0.038 meters as compared to the classified LAS, and 0.047 meters against the bare earth DEM, with 95% confidence (Figure 6 and Figure 7).

NV5 also assessed absolute accuracy using 9 ground control points. Although these points were used in the calibration and post-processing of the lidar point cloud, they still provide a good indication of the overall accuracy of the lidar dataset, and therefore have been provided in Table 14 and Figure 8.

---

<sup>1</sup> Federal Geographic Data Committee, ASPRS POSITIONAL ACCURACY STANDARDS FOR DIGITAL GEOSPATIAL DATA EDITION 1, Version 1.0, NOVEMBER 2014.

[https://www.asprs.org/a/society/committees/standards/Positional\\_Accuracy\\_Standards.pdf](https://www.asprs.org/a/society/committees/standards/Positional_Accuracy_Standards.pdf).

**Table 14: Absolute accuracy results**

Absolute Vertical Accuracy			
	NVA, as compared to Classified LAS	NVA, as compared to Bare Earth DEM	Ground Control Points
Sample	48 points	48 points	9points
95% Confidence (1.96*RMSE)	0.038 m	0.047 m	0.022 m
Average	-0.007 m	-0.011 m	-0.002 m
Median	-0.008 m	-0.011 m	-0.006 m
RMSE	0.019 m	0.024 m	0.011 m
Standard Deviation (1σ)	0.018 m	0.021 m	0.011 m

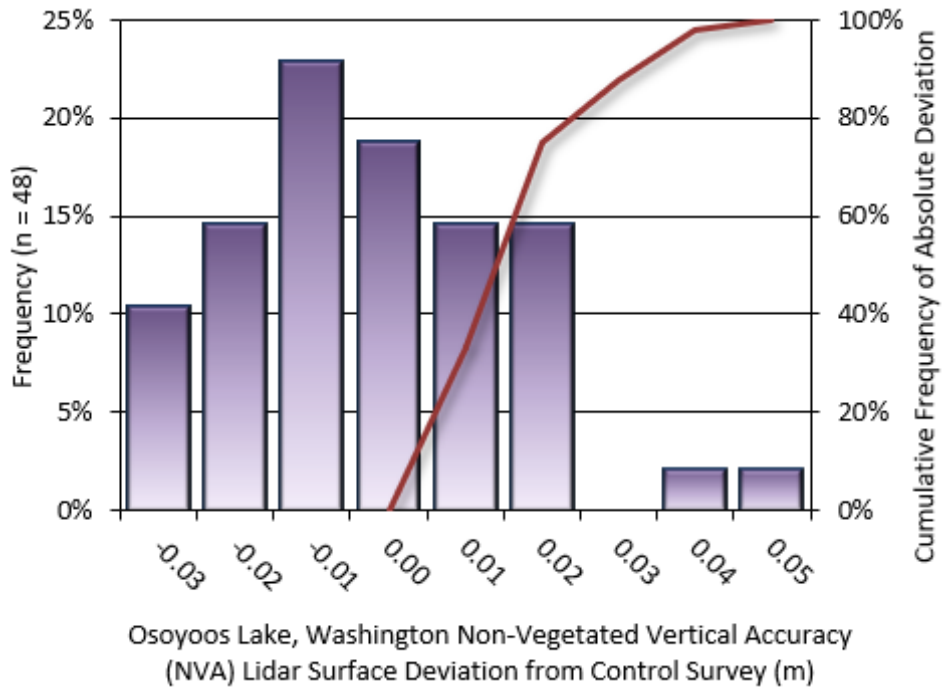


**Figure 6: Frequency histogram for classified LAS deviation from ground check point values**

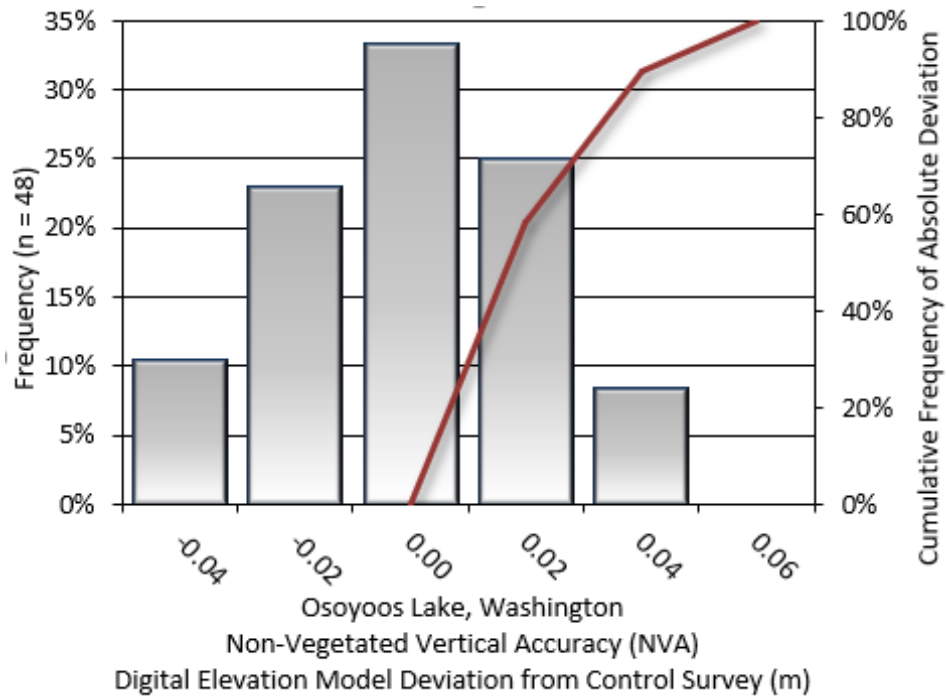


**Figure 7: Frequency histogram for lidar bare earth DEM deviation from ground check point values**

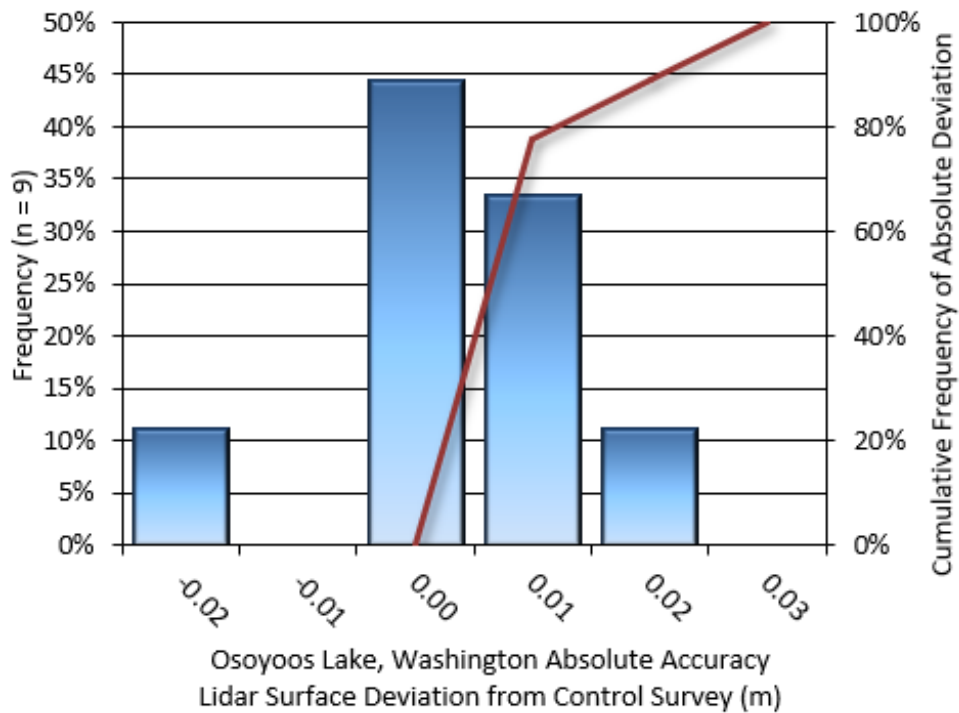


**Figure 8: Frequency histogram for lidar surface deviation ground control point values**

## Lidar Bathymetric Vertical Accuracies

Traditional bathymetric (submerged and along the water’s edge) check points were collected in order to assess the submerged surface vertical accuracy. Additionally NV5 ground survey staff placed submerged shallow and deep water physical targets throughout the AOI to further assess the depth accuracy of the two Leica topbathy sensors. Assessment of 50 submerged bathymetric check points resulted in a vertical accuracy of 0.072 meters, while assessment of 15 wetted edge check points resulted in a vertical accuracy of 0.094 meters, evaluated at 95% confidence interval (Table 15, Figure 9, Figure 10). Assessment of the submerged underwater targets resulted in a vertical accuracy of 0.046 meters evaluated at the 95% confidence level (Table 15 and Figure 11).

**Table 15: Bathymetric Vertical Accuracy for the Osoyoos Lake Project**

Bathymetric Vertical Accuracy			
	Submerged Bathymetric Check Points	Wetted Edge Bathymetric Check Points	Submerged Shallow Water Targets
Sample	50 points	15 points	4 targets
95% Confidence (1.96*RMSE)	0.072 m	0.094 m	0.046 m
Average Dz	0.015 m	0.003 m	-0.002 m
Median	0.017 m	-0.003 m	0.001 m
RMSE	0.037 m	0.048 m	0.023 m
Standard Deviation (1σ)	0.034 m	0.050 m	0.027 m

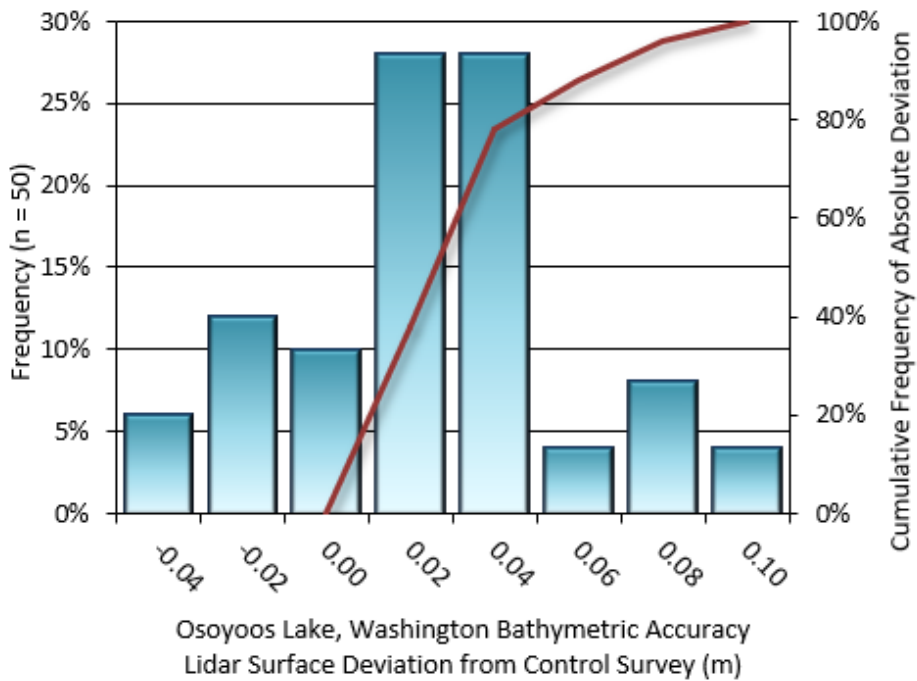


Figure 9: Frequency histogram for lidar surface deviation from submerged check point values

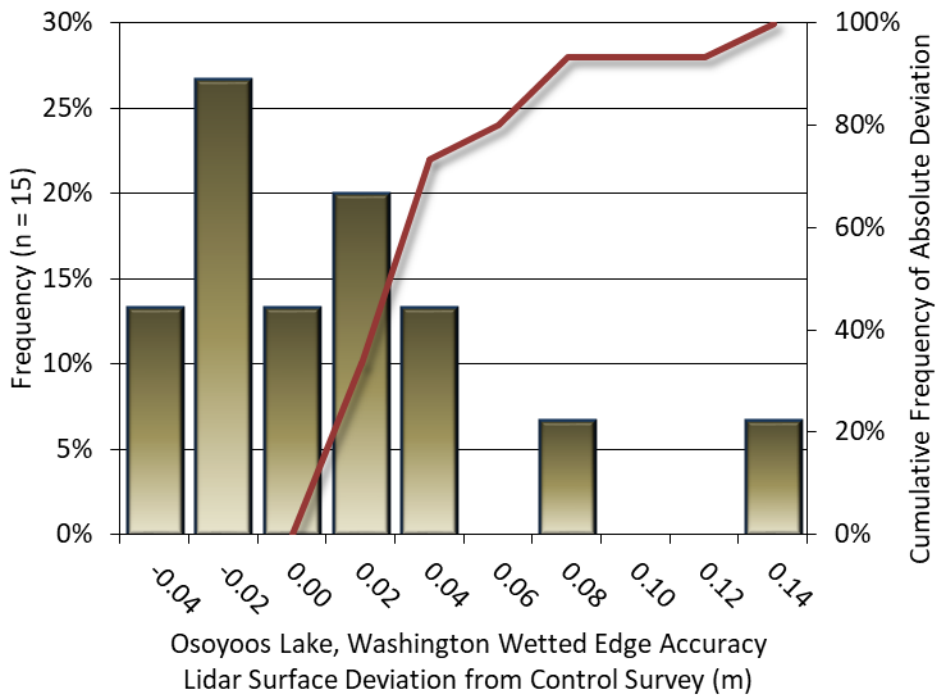
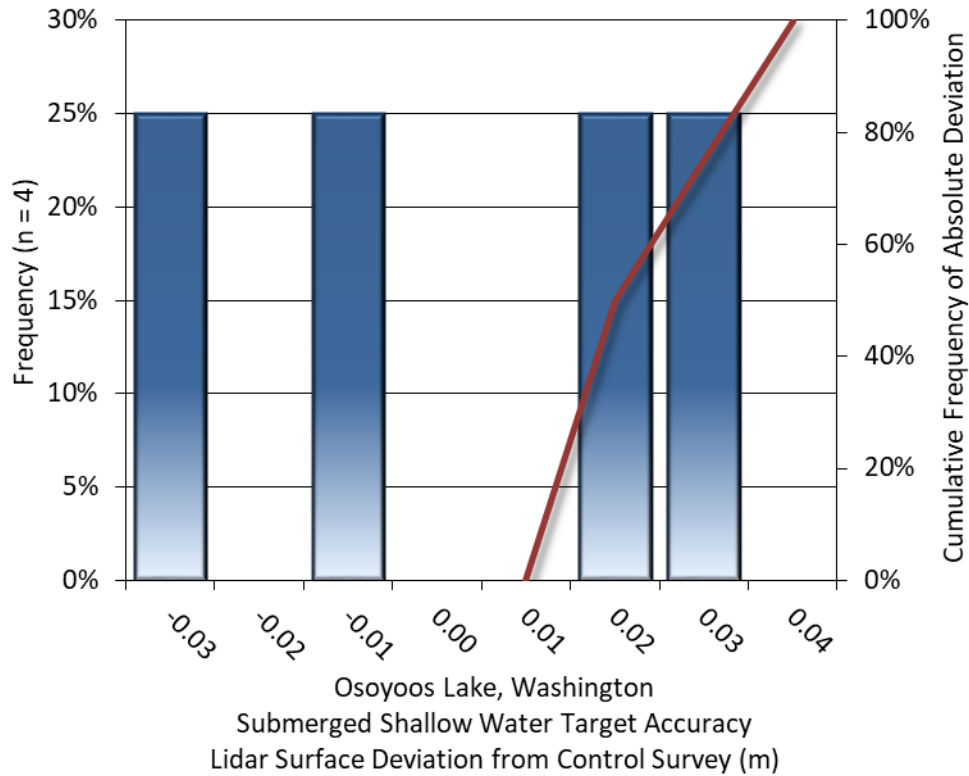


Figure 10: Frequency histogram for lidar surface deviation from wetted edge check point values



**Figure 11: Frequency histogram for lidar surface deviation from shallow water target values**

## Lidar Vegetated Vertical Accuracies

NV5 also assessed vertical accuracy using Vegetated Vertical Accuracy (VVA) reporting. VVA compares known ground check point data collected over vegetated surfaces using land class descriptions to the triangulated ground surface generated by the ground classified lidar points. VVA is evaluated at the 95<sup>th</sup> percentile (Table 16, Figure 12, Figure 13).

**Table 16: Vegetated Vertical Accuracy for the Osoyoos Lake Project**

Vegetated Vertical Accuracy (VVA)		
	VVA, as compared to Classified LAS	VVA, as compared to Bare Earth DEM
Sample	18 points	18 points
Average Dz	0.038 m	0.028 m
Median	0.035 m	0.018 m
RMSE	0.054 m	0.043 m
Standard Deviation (1σ)	0.039 m	0.034 m
95 <sup>th</sup> Percentile	0.091 m	0.084 m

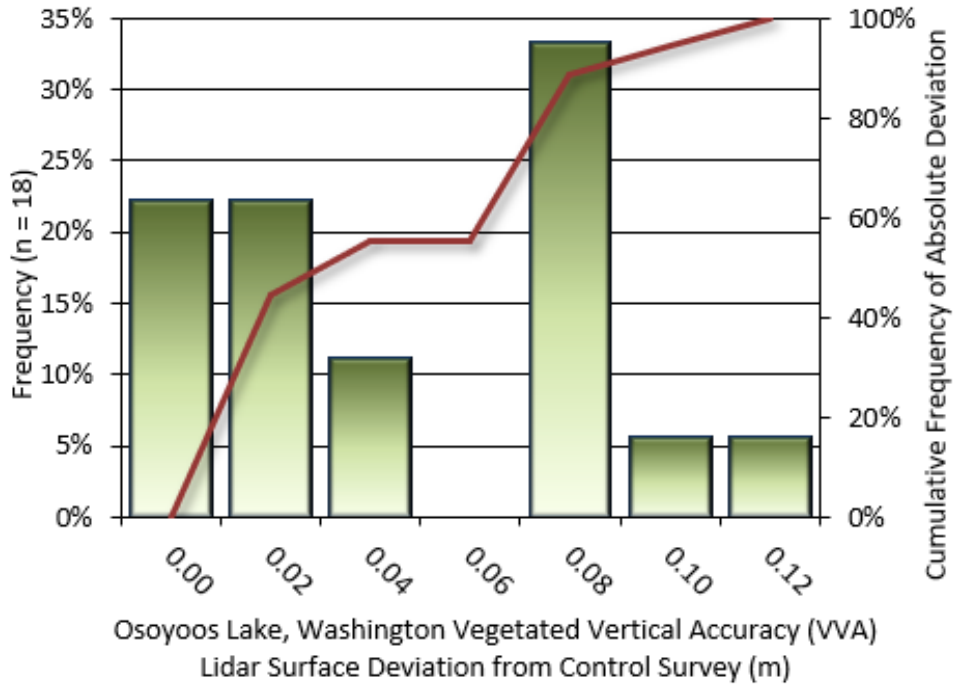


Figure 12: Frequency histogram for lidar surface deviation from all land cover class point values (VVA)

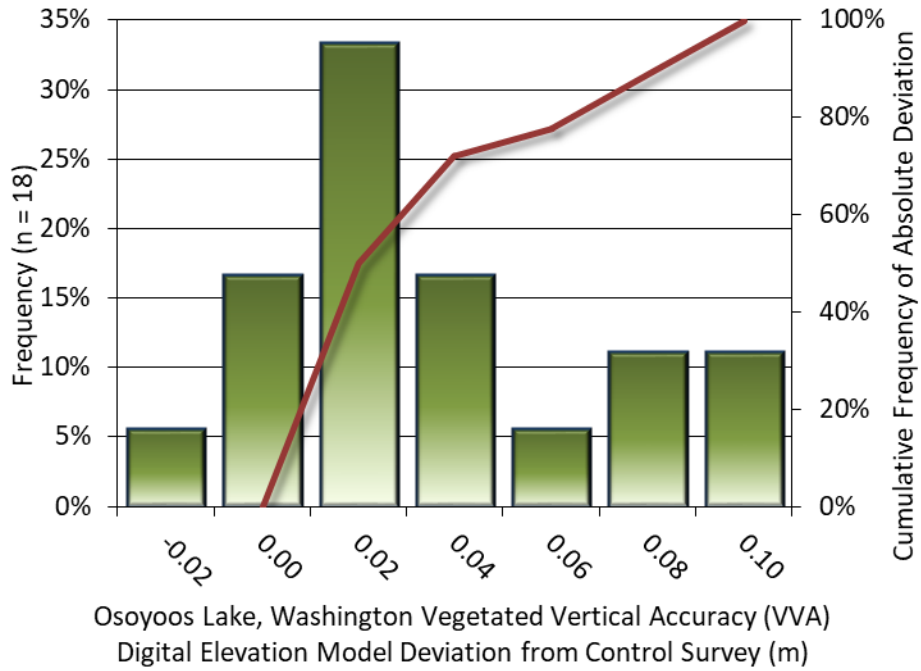


Figure 13: Frequency histogram for lidar surface deviation from all land cover class point values (VVA)

## Lidar Relative Vertical Accuracy

Relative vertical accuracy refers to the internal consistency of the data set as a whole: the ability to place an object in the same location given multiple flight lines, GPS conditions, and aircraft attitudes. When the lidar system is well calibrated, the swath-to-swath vertical divergence is low (<0.10 meters). The relative vertical accuracy was computed by comparing the ground surface model of each individual flight line with its neighbors in overlapping regions. The average (mean) line to line relative vertical accuracy for the Osoyoos Lake Lidar project was 0.041 meters (Table 17, Figure 14).

**Table 17: Relative accuracy results**

Relative Accuracy	
Sample	86 surfaces
Average	0.041 m
Median	0.039 m
RMSE	0.046 m
Standard Deviation ( $1\sigma$ )	0.016 m
1.96 $\sigma$	0.031 m

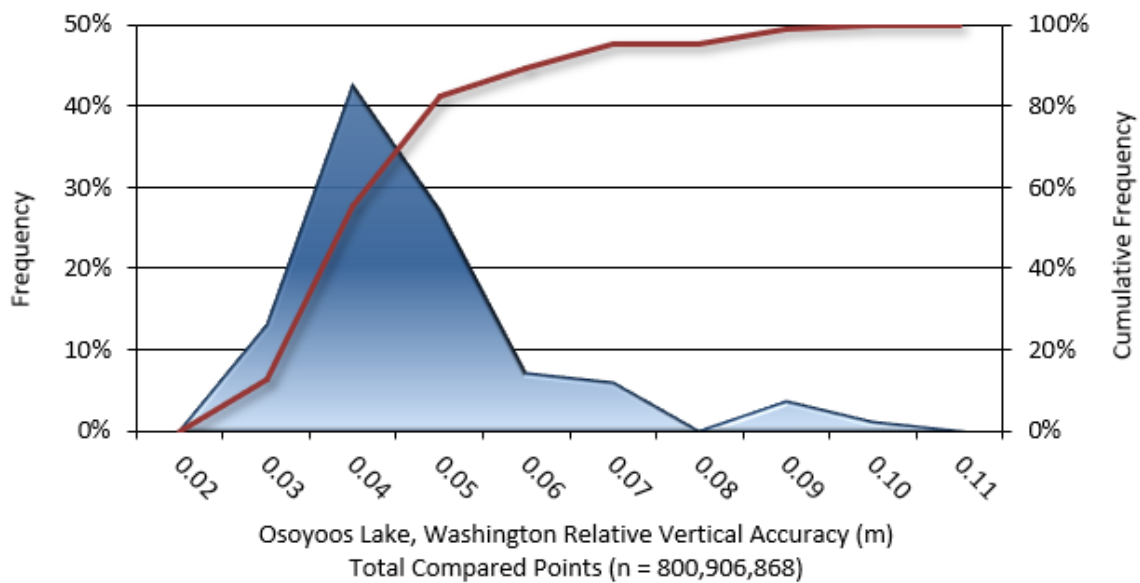


**Figure 14: Frequency plot for relative vertical accuracy between flight lines**

## Lidar Horizontal Accuracy

Lidar horizontal accuracy is a function of Global Navigation Satellite System (GNSS) derived positional error, flying altitude, and INS derived attitude error. The obtained  $RMSE_r$  value is multiplied by a conversion factor of 1.7308 to yield the horizontal component of the National Standards for Spatial Data Accuracy (NSSDA) reporting standard where a theoretical point will fall within the obtained radius 95 percent of the time. Based on a flying altitude of 500 meters, an IMU error of 0.002 decimal degrees, and a GNSS positional error of 0.005 meters, this project was produced to 0.05 m horizontal accuracy at the 95% confidence level.

**Table 18: Horizontal Accuracy**

Horizontal Accuracy	
$RMSE_r$	0.03 m
$ACC_r$	0.05 m

# Photo Analytical Aerial Triangulation Report

## Overview

Aerial triangulation was performed in one block to support photogrammetric mapping efforts of the Osoyoos Lake in northern Washington. The block consisted of four flight lines of 87 images flown at a scale of 1:800 on September 16<sup>th</sup>, 2021. Block adjustments were made to ground control established by NV5 referencing UTM11N, NAD83(CSRS)V4e2002 horizontal datum and CGVD 2013 vertical datum, however final orthophoto products were transformed to NAD83(2011) horizontal datum using a horizontal datum shift. Digital imagery along with ground control and camera calibration data were used as input to Inpho’s Match AT softcopy photogrammetry program. The sensor used was a Leica DMC III, large format, aerial mapping camera. Of the 27 total surveyed air target points, 16 were used for aerial triangulation and 10 were withheld from the block adjustment as check points for accuracy assessment, remaining air target points were either deemed misfits or redundant due to their proximity to other ground control.

## Control Points

Air target points used in the aerial triangulation adjustment are listed with their location in Table 19, and RMSE values can be found in Table 20.

**Table 19: Location of air target points used as control for aerial triangulation adjustment**

Control Point Coordinates (m) – 16 Total Points				Control Point Residuals (m) - 16 Total Points			
Point ID	X	Y	Z	X	Y	Z	Block ID
AT047	317163.577	5426940.135	404.054	0.007	-0.034	0.078	Osoyoos Lake
AT048	317162.867	5426939.545	404.026	-0.027	0.040	0.129	Osoyoos Lake
AT049	317162.972	5426940.819	403.999	-0.008	-0.012	0.060	Osoyoos Lake
AT050	318598.657	5425236.363	358.201	0.023	-0.030	0.078	Osoyoos Lake
AT051	318598.320	5425233.956	358.193	-0.004	-0.005	0.139	Osoyoos Lake
AT139	320967.923	5433667.653	279.832	-0.029	0.033	-0.031	Osoyoos Lake
AT140	320967.314	5433667.660	279.865	-0.030	0.047	0.004	Osoyoos Lake
AT141	320967.282	5433670.840	279.902	-0.042	0.025	-0.036	Osoyoos Lake
AT142	315137.190	5438875.045	285.460	-0.046	0.038	-0.090	Osoyoos Lake
AT150	322693.601	5421375.323	286.586	0.025	0.020	0.020	Osoyoos Lake
AT152	322204.283	5418406.005	289.151	0.029	-0.001	0.010	Osoyoos Lake
AT154	322006.769	5422431.030	280.731	0.034	0.005	-0.085	Osoyoos Lake
AT155	322009.033	5422422.216	280.858	0.024	-0.036	-0.065	Osoyoos Lake
AT158	320613.006	5429654.764	279.847	0.031	-0.005	-0.112	Osoyoos Lake
AT162	321936.957	5424797.172	279.044	0.008	-0.040	-0.058	Osoyoos Lake
AT164	321939.141	5424795.877	279.021	0.006	-0.042	-0.041	Osoyoos Lake

**Table 20: RMSE for air target points used as control for aerial triangulation adjustment**

Control Point RMSE - 16 Total Points		
Meters		
X	Y	Z
0.027	0.03	0.076

## Check Points

Air target check points withheld from the aerial triangulation adjustment are listed with their location and residuals in Table 21, RMSE values can be found in

Table 22.

**Table 21: Location of air target check points withheld from aerial triangulation adjustment**

Check Point Coordinates (m) - 10 Total Points				Check Point Residuals (m) -10 Total Points			
Point ID	X	Y	Z	X	Y	Z	Block ID
AT052	318546.820	5425260.065	354.089	0.063	-0.047	0.100	Osoyoos Lake
AT138	320974.550	5433660.563	279.579	0.016	0.111	-0.020	Osoyoos Lake
AT143	315109.838	5438860.827	285.461	-0.133	0.118	-0.232	Osoyoos Lake
AT151	322693.814	5421368.472	286.722	-0.040	0.047	0.016	Osoyoos Lake
AT153	322205.114	5418414.857	289.256	-0.009	0.079	-0.074	Osoyoos Lake
AT156	321240.204	5426387.719	280.412	0.032	-0.029	-0.204	Osoyoos Lake
AT157	321248.173	5426394.623	280.118	-0.026	0.009	-0.132	Osoyoos Lake
AT159	320609.139	5429674.017	280.338	0.014	0.044	0.030	Osoyoos Lake
AT160	322144.155	5428876.231	279.718	-0.207	0.047	0.160	Osoyoos Lake
AT163	321939.539	5424801.899	279.004	-0.013	-0.088	-0.068	Osoyoos Lake

**Table 22: RMSE for air target points withheld from aerial triangulation adjustment**

Check Point RMSE - 10 Total Points		
Meters		
X	Y	Z
0.083	0.071	0.127

## Anomalies and Misfits

One ATP was omitted from processing due to its close proximity to other ATPs. ATP redundancy can be useful when points fails QAQC measures or are obscured by shadow or object lean.

## CERTIFICATIONS

NV5 Geospatial provided lidar services for the Osoyoos Lake project as described in this report.

I, Shauna Gutierrez, have reviewed the attached report for completeness and hereby state that it is a complete and accurate report of this project.

*Shauna Gutierrez*  
Shauna Gutierrez (Mar 9, 2022 16:38 PST)

Mar 9, 2022

Shauna Gutierrez  
Project Manager  
NV5 Geospatial

I, Evon P. Silvia, PLS, being duly registered as a Professional Land Surveyor in and by the state of Washington, hereby certify that the methodologies, static GNSS occupations used during airborne flights, and ground survey point collection were performed using commonly accepted Standard Practices. Field work conducted for this report was conducted on September 14-29, 2021.

Accuracy statistics shown in the Accuracy Section of this Report have been reviewed by me and found to meet the “National Standard for Spatial Data Accuracy”.

*Evon P. Silvia* Mar 9, 2022

Evon P. Silvia, PLS  
NV5 Geospatial  
Corvallis, OR 97330



## SELECTED IMAGES



**Figure 15: A view looking east over the Similkameen and Okanogan rivers, about 14 miles north of Tonasket and 3 miles south of Oroville near the Whistler Canyon Trailhead. This image was created from the lidar bare earth surface colored by elevation.**

# GLOSSARY

**1-sigma ( $\sigma$ ) Absolute Deviation:** Value for which the data are within one standard deviation (approximately 68<sup>th</sup> percentile) of a normally distributed data set.

**1.96 \* RMSE Absolute Deviation:** Value for which the data are within two standard deviations (approximately 95<sup>th</sup> percentile) of a normally distributed data set, based on the FGDC standards for Non-vegetated Vertical Accuracy (FVA) reporting.

**Accuracy:** The statistical comparison between known (surveyed) points and laser points. Typically measured as the standard deviation ( $\sigma$ ) and root mean square error (RMSE).

**Absolute Accuracy:** The vertical accuracy of lidar data is described as the mean and standard deviation ( $\sigma$ ) of divergence of lidar point coordinates from ground survey point coordinates. To provide a sense of the model predictive power of the dataset, the root mean square error (RMSE) for vertical accuracy is also provided. These statistics assume the error distributions for x, y and z are normally distributed, and thus we also consider the skew and kurtosis of distributions when evaluating error statistics.

**Relative Accuracy:** Relative accuracy refers to the internal consistency of the data set; i.e., the ability to place a laser point in the same location over multiple flight lines, GPS conditions and aircraft attitudes. Affected by system attitude offsets, scale and GPS/IMU drift, internal consistency is measured as the divergence between points from different flight lines within an overlapping area. Divergence is most apparent when flight lines are opposing. When the lidar system is well calibrated, the line-to-line divergence is low (<10 cm).

**Root Mean Square Error (RMSE):** A statistic used to approximate the difference between real-world points and the lidar points. It is calculated by squaring all the values, then taking the average of the squares and taking the square root of the average.

**Data Density:** A common measure of lidar resolution, measured as points per square meter.

**Digital Elevation Model (DEM):** File or database made from surveyed points, containing elevation points over a contiguous area. Digital terrain models (DTM) and digital surface models (DSM) are types of DEMs. DTMs consist solely of the bare earth surface (ground points), while DSMs include information about all surfaces, including vegetation and man-made structures.

**Intensity Values:** The peak power ratio of the laser return to the emitted laser, calculated as a function of surface reflectivity.

**Nadir:** A single point or locus of points on the surface of the earth directly below a sensor as it progresses along its flight line.

**Overlap:** The area shared between flight lines, typically measured in percent. 100% overlap is essential to ensure complete coverage and reduce laser shadows.

**Pulse Rate (PR):** The rate at which laser pulses are emitted from the sensor; typically measured in thousands of pulses per second (kHz).

**Pulse Returns:** For every laser pulse emitted, the number of wave forms (i.e., echoes) reflected back to the sensor. Portions of the wave form that return first are the highest element in multi-tiered surfaces such as vegetation. Portions of the wave form that return last are the lowest element in multi-tiered surfaces.

**Real-Time Kinematic (RTK) Survey:** A type of surveying conducted with a GPS base station deployed over a known monument with a radio connection to a GPS rover. Both the base station and rover receive differential GPS data and the baseline correction is solved between the two. This type of ground survey is accurate to 1.5 cm or less.

**Post-Processed Kinematic (PPK) Survey:** GPS surveying is conducted with a GPS rover collecting concurrently with a GPS base station set up over a known monument. Differential corrections and precisions for the GNSS baselines are computed and applied after the fact during processing. This type of ground survey is accurate to 1.5 cm or less.

**Scan Angle:** The angle from nadir to the edge of the scan, measured in degrees. Laser point accuracy typically decreases as scan angles increase.

**Native Lidar Density:** The number of pulses emitted by the lidar system, commonly expressed as pulses per square meter.

## APPENDIX A - ACCURACY CONTROLS

### Relative Accuracy Calibration Methodology:

**Manual System Calibration:** Calibration procedures for each mission require solving geometric relationships that relate measured swath-to-swath deviations to misalignments of system attitude parameters. Corrected scale, pitch, roll and heading offsets were calculated and applied to resolve misalignments. The raw divergence between lines was computed after the manual calibration was completed and reported for each survey area.

**Automated Attitude Calibration:** All data was tested and calibrated using TerraMatch and StripAlign automated sampling routines. Ground points were classified for each individual flight line and used for line-to-line testing. System misalignment offsets (pitch, roll and heading) and scale were solved for each individual mission and applied to respective mission datasets. The data from each mission were then blended when imported together to form the entire area of interest.

**Automated Z Calibration:** Ground points per line were used to calculate the vertical divergence between lines caused by vertical GPS drift. Automated Z calibration was the final step employed for relative accuracy calibration.

### Lidar accuracy error sources and solutions:

Type of Error	Source	Post Processing Solution
GPS (Static/Kinematic)	Long Base Lines	None
	Poor Satellite Constellation	None
	Poor Antenna Visibility	Reduce Visibility Mask
Relative Accuracy	Poor System Calibration	Recalibrate IMU and sensor offsets/settings
	Inaccurate System	None
Laser Noise	Poor Laser Timing	None
	Poor Laser Reception	None
	Poor Laser Power	None
	Irregular Laser Shape	None

### Operational measures taken to improve relative accuracy:

**Low Flight Altitude:** Terrain following was employed to maintain a constant above ground level (AGL). Laser horizontal errors are a function of flight altitude above ground (about 1/3000<sup>th</sup> AGL flight altitude).

**Focus Laser Power at narrow beam footprint:** A laser return must be received by the system above a power threshold to accurately record a measurement. The strength of the laser return (i.e., intensity) is a function of laser emission power, laser footprint, flight altitude and the reflectivity of the target. While surface reflectivity cannot be controlled, laser power can be increased and low flight altitudes can be maintained.

**Reduced Scan Angle:** Edge-of-scan data can become inaccurate. The scan angle was reduced to a maximum of  $\pm 20^\circ$  from nadir, creating a narrow swath width and greatly reducing laser shadows from trees and buildings.

**Quality GPS:** Flights took place during optimal GPS conditions (e.g., 6 or more satellites and PDOP [Position Dilution of Precision] less than 3.0). Before each flight, the PDOP was determined for the survey day. During all flight times, a dual frequency DGPS base station recording at 1 second epochs was utilized and a maximum baseline length between the aircraft and the control points was less than 13 nm at all times.

**Ground Survey:** Ground survey point accuracy (<1.5 cm RMSE) occurs during optimal PDOP ranges and targets a minimal baseline distance of 4 miles between GPS rover and base. Robust statistics are, in part, a function of sample size (n) and distribution. Ground survey points are distributed to the extent possible throughout multiple flight lines and across the survey area.

**50% Side-Lap (100% Overlap):** Overlapping areas are optimized for relative accuracy testing. Laser shadowing is minimized to help increase target acquisition from multiple scan angles. Ideally, with a 50% side-lap, the nadir portion of one flight line coincides with the swath edge portion of overlapping flight lines. A minimum of 50% side-lap with terrain-followed acquisition prevents data gaps.

**Opposing Flight Lines:** All overlapping flight lines have opposing directions. Pitch, roll and heading errors are amplified by a factor of two relative to the adjacent flight line(s), making misalignments easier to detect and resolve.









# IJC\_Osoyoos\_Topobathymetric\_Lidar\_Report

Final Audit Report

2022-03-10

Created:	2022-03-10
By:	Drew carey (Drew.Carey@nv5.com)
Status:	Signed
Transaction ID:	CBJCHBCAABAAydVzG8VKc_wl4IDfvyhACaajvwk5P2Q7

## "IJC\_Osoyoos\_Topobathymetric\_Lidar\_Report" History

-  Document created by Drew carey (Drew.Carey@nv5.com)  
2022-03-10 - 0:17:47 AM GMT- IP address: 50.237.124.180
-  Document emailed to Evon Silvia (evon.silvia@nv5.com) for signature  
2022-03-10 - 0:31:27 AM GMT
-  Email viewed by Evon Silvia (evon.silvia@nv5.com)  
2022-03-10 - 0:36:56 AM GMT- IP address: 50.237.124.180
-  Document e-signed by Evon Silvia (evon.silvia@nv5.com)  
Signature Date: 2022-03-10 - 0:37:22 AM GMT - Time Source: server- IP address: 50.237.124.180
-  Document emailed to Shauna Gutierrez (shauna.gutierrez@nv5.com) for signature  
2022-03-10 - 0:37:24 AM GMT
-  Email viewed by Shauna Gutierrez (shauna.gutierrez@nv5.com)  
2022-03-10 - 0:37:44 AM GMT- IP address: 213.188.67.191
-  Document e-signed by Shauna Gutierrez (shauna.gutierrez@nv5.com)  
Signature Date: 2022-03-10 - 0:38:24 AM GMT - Time Source: server- IP address: 50.237.124.180
-  Agreement completed.  
2022-03-10 - 0:38:24 AM GMT